Particularities of Cu and Zn Nanoparticles Formation in a Magnetic Field

Vyacheslav F. Myshkin[1,a], Valeriy A. Khan[1,2], Milan Tichy[1,3], Anna Kapran[3],
Dmitriy A. Izhoykin[4], Vladimir N. Lenskiy[1], Denis L. Gamov[1]
and Darya A. Leonteva[1]

[1]*Tomsk Polytechnic University, 30 Lenina Av., 634050, Tomsk, Russian Federation*
[2]*V.E. Zuev Institute of Atmospheric Optics SB RAS, 1 Akademicheski Av., 634055, Tomsk, Russian Federation*
[3]*Charles University, Faculty of Mathematics and Physics, 2 V Holešovičkách, 180 00 Praha 8, Czech Republic*
[4]*Tomsk State University of Architecture and Building, 2 Solyanaya Sq., 634003, Tomsk, Russian Federation*

[a]Corresponding author: gos100@tpu.ru

Abstract. We studied experimentally the condensation of Zn and Cu vapors from a high-temperature gas in an external weak constant magnetic field. We observed at all applied conditions, a chaotic time shift of the maximum of the size distribution function of dispersed particles. Simultaneously, a decrease in the width of the size distribution function of dispersed Zn particles from 40 nm (0 mT) to 10 nm (44 mT or 76 mT) was observed. The sizes of Zn particles were determined by laser probing. The sizes of dispersed Cu particles, determined by analyzing a substrate sample, were in the range of 10–400 nm without a magnetic field, and the range 30–320 nm in a magnetic field of 30 mT. The authors explain the observed results by arranging the dynamics of the spin pair of unpaired electrons of an atom from the gas phase and of an atom on the surface of a condensed particle in a magnetic field. Therefore, in a magnetic field, when an atom collides with a dispersed particle or condensation nucleus, the probability of creation of a singlet pair of spins of unpaired electrons is higher than that without a field.

INTRODUCTION

The magnetic field enables changing the deposition rate, uniformity, structure and physico-chemical properties of films obtained by an electrochemical process. In [1], the action of a magnetic field (12 T) during electrodeposition was associated with magnetohydrodynamic convection. To obtain information on the kinetics of the formation of deposits by electrochemical processes, the authors analyzed in [1] the transients of the flux density for several materials and compared their results with the data of other authors [2, 3]. The nucleation rates of a Ni film in a magnetic field of up to 0.7 T also significantly increase when the natural and additional convection created by the magnetic field acts in the same direction [4]. When Ni is deposited in a magnetic field of 0.7 T, smaller crystals are formed than without a field.

The results obtained in [1-4] may be explained by the rearrangement of atoms at the solid-liquid interface due to the magnetic field [5]. The movement of water molecules near the solid-liquid interface in a magnetic field is affected by the Lorentz force, which causes unstable or metastable atoms, which fall on the surface of a solid at the interface, to migrate to stable positions.

Laser ablation of particles in a liquid in a magnetic field of 7.5 T reduces their size from 8 nm to 3 nm, and their shape becomes spherical [6]. The obtained experimental results are explained by the fact that at the intensity of the laser radiation used the laser breakdown plasma is formed in the described experiments ($\approx 10^{10}$ W/cm^2) [7]. The magnetic field leads to a significant increase of the plasma lifetime [8]. The presence of smaller particles than the initial ones is explained by the authors as a result of condensation of the material from the plasma torch [9].

Phase transitions and chemical reactions are associated with the formation or destruction of molecular

(intermolecular) bonds formed by paired electrons. The valence electron and the nuclei of some isotopes have a magnetic moment (spin) involved in magnetic interactions. Therefore, in order to analyze the dependence of the phase transition rate on the magnetic field, we take into account the dynamics of spin pairs of unpaired electrons of interacting atoms using the previously estimated uncertainty of the spin precession phase in a magnetic field [10].

The formation of an aerosol without a magnetic field is widely studied. For example, the work [11] discusses the features of the dynamics of an aerosol formed from a plasma during welding operations. The primary aerosol formed because of nucleation and growth has two modes with average sizes of 2 and 10 nm. At coagulation of particles with an average size of 10 nm, positively charged clusters appear, having an average size of ~ 200 nm. Coagulation of particles with an average diameter of 2 nm occurs in two stages: first the negatively charged agglomerates form during a period of 0.1 μs, which are then combined with clusters originating from particles with an average size of 10 nm. As a result, new agglomerates with an average size of ~ 300 nm appear. Consequently, an aerosol with a bimodal size distribution is formed. Thus, in a high-temperature system, various phenomena are involved in the formation of a spectrum of sizes of the dispersed phase.

The nucleation process begins with the collision of three particles and the formation of condensation nuclei — clusters of atoms. At low supersaturation, clusters can spontaneously evaporate. The frequency of the fluctuation formation of condensation nuclei is established in a time less than 1 ns. The theory of fluctuations determines the rate of the seed formation of a new phase in a unit volume of supersaturated steam [12]:

$$\frac{dN}{d\tau} = \frac{\gamma}{\rho} \sqrt{\frac{2m\sigma}{\pi}} \left(\frac{P}{kT}\right)^2 \exp\left(-\frac{\Delta G}{kT}\right),$$ (1)

where N is the concentration of droplets, cm^{-3}; τ - time, s; γ - the coefficient of desublimation; ρ - the sublimate density, kg/cm^3; m - the mass of a vapor molecule, kg; $k = 1.38\times10^{-23}$ J/K the Boltzmann constant; P - the total pressure of the vapor-gas mixture, mm Hg; T - the temperature of the mixture, K; ΔG - the energy of droplet formation, σ - the coefficient of surface tension [13].

The value of γ expresses the fraction of vapor molecules remaining after collisions on a solid surface ($\gamma \in 0 \div 1.0$). For a spherical drop in a supersaturated vapor, the total energy of formation is determined by [13, 14]:

$$\Delta G = \frac{16\pi \, m^2 \sigma^3}{3\rho^2 k^2 T^2 (\ln S)}.$$ (2)

High-temperature processes are widely used in various technologies: surface treatment [15, 16], processing of powders and waste [17], separation of isotopes [10], obtaining powders of refractory materials [18]. At present, however, insufficient attention is paid to the possibility to control the sizes of dispersed particles of diamagnetic substances formed from the high-temperature state by the constant magnetic field.

The purpose of this study is to determine the possibility of influencing/control of the sizes of dispersed particles of Cu and Zn, formed when cooling atomic vapors at a weak constant magnetic field.

EXPERIMENTAL FACILITY

When studying the effect of an external constant magnetic field on the process of formation of the dispersed particles we estimated the granulometric composition of the resulting nanoparticles. For determination of the particle sizes, we applied scanning electron microscopy (SEM) and the spectral transparency method.

At the first facility, the evaporator, we studied the phase transition from the high-temperature flow. The simplified scheme of the evaporator system shows Fig. 1a. Zinc has evaporated from a cylindrical bath with an outer diameter of 16 mm and a height of 20 mm made of non-magnetic stainless steel that was placed in a cylindrical heater.

We have used the granular zinc brand "analytical grade" - pure for analysis according RF Technical Requirements # 6-09-5294-86. The heater was a ceramic tube with an internal diameter of 18 mm with a NiCr wire wound outside. To prevent oxidation of zinc vapor the high-purity argon gas (99.998% following the RF Technical Requirements # 6-21-12-94) flew between the heater and the bath, as well as between the heater and the outer case (not shown in Fig.1a). The heater was accommodated in a heat insulating housing, the internal diameter of which did not exceed 30 mm. With the help of the Comsol Program we modeled the steam–gas flow with a temperature of 950° C formed over the bath. The design of the evaporator system followed the calculation results, and it prevented contact and subsequent cooling of the steam-gas flow containing Zn vapors and Zn nanoparticles by cold air. The

magnetic field was formed by two permanent magnets, 3×5 cm in size, with a residual magnetization of 1.1 T and encompassed the whole region of Zn evaporation and vapor cooling. The magnitude of the magnetic field was altered by changing the distance between the magnets and monitored using a magnetic meter ATE-8702 (Aktakom), with the resolution of 0.01 mT. Heat insulators 2 mm thick were installed between permanent magnets and hot surfaces.
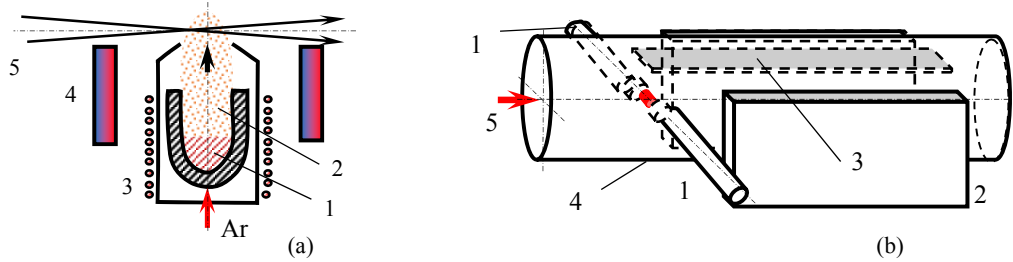
FIGURE 1. Scheme of experimental facilities for the formation of dispersed particles from a high-temperature flow containing vapors of metals: a) zinc: 1 – zinc melt, 2 - zinc vapors, 3 – heater, 4 – permanent magnets, 5 – probing laser beam; b) copper: 1 – arc electrodes, 2 – permanent magnets, 3 – substrate, 4 – quartz tube, 5 – argon flow.

The heterogeneous flux at the output of the heater was shined through at its cross-section by a beam of radiation in the wavelength range of 420–650 nm generated by a LED made in China. We assumed that the aerosol stream had a cylindrical geometry, through the center of which passed a probing beam of optical radiation. The LED converted part of the primary radiation into the long-wavelength region by a special layer. Therefore, in the emission spectrum of the used LED, we found two maxima at the wavelengths around 455 nm and 555 nm (Fig. 2). The observed "periodic variation" of the intensity of the longer-wave peak was associated with the specifics of the conversion of the light flux by the photosensitive matrix of the SL-140 spectrometer produced by the Solar TII, Ltd. Co. The spectrum of the probing radiation transmitted through a heterogeneous flux was recorded using an SL-140 spectrometer with the resolution 0.27 nm.

In the second facility, shown in Fig.1b, we created an arc discharge in a cylindrical chamber made of quartz glass produced with accord to RF Technical Requirements # 5932-014-0028-8679-01, through which high-purity argon was pumped at a rate of 1 standard l/s. Copper electrodes with a diameter of 4 mm were arranged radially at an angle of 10-15° to the horizontal axis of the chamber. A 1.5 kW transformer with an open circuit voltage of 5 kV was used to power the arc. When the distance between the electrodes was 5-6 mm, the arc current did not exceed 18 A. To initiate the electric arc, the electrodes were mechanically brought into contact for a little moment.
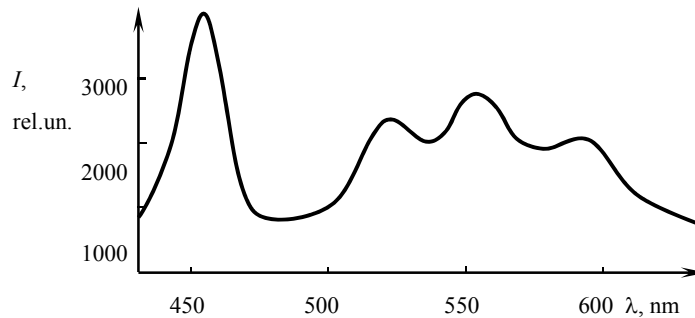
FIGURE 2. The spectrum of the probing light.

The substrate for the deposition of dispersed particles was placed at a distance of 1 cm from the electrodes along the axis of the chamber and at a height of 1.5 cm above the arc. Two permanent magnets, 9×12 cm in size, were mounted outside the chamber towards each other at a distance of 3 mm from the chamber surface. Each magnet separately created a magnetic field of 230 mT at a distance of 3 mm from its surface. The magnitude of the magnetic field was determined by the distance between the permanent magnets fixed in special holders. The external magnetic field was oriented along the electric arc and contributed to its stabilization in space. The arc electrodes were partly covered by quartz tubes to prevent spontaneous spreading of the arc over all the electrode length. Metal then evaporated only from the open parts of the copper electrodes. Quartz also evaporated, but at a much slower pace.

RESULTS AND DISCUSSION

We first consider the results obtained with the first facility. In each series of measurements, we recorded 15–30 spectra during the evaporation time of 2-3 grams of Zn. We observed a fluctuation in vapor concentration. The transmittance was determined as the ratio of the intensity of the radiation transmitted through a heterogeneous flux to the intensity of radiation without dispersed particles at each wavelength. An external constant magnetic field with induction of 44 mT and 76 mT was used. The effect of the magnetic field created by the heater winding is included in these figures.

Figure 3a shows the spectral course of the transmittance of dispersed Zn particles formed in a constant magnetic field of 76 mT for one measurement series. It is evident that the graphs of the dependencies have mainly linear character in the wavelength range 420-650 nm. In the spectral range 420-650 nm, however, the graphs slightly deviate from the linear dependence. The repeated observations in a magnetic field revealed that the graphs of the spectral course of the transmittance are almost parallel for different values of the transmittance k. Without a magnetic field, the spectral plots can intersect due to significant differences in optical densities in the wavelength range from 420 nm to 650 nm.

To determine the size distribution function of dispersed Zn particles, the spectral course of transmission coefficients was processed using the regularizing algorithms for solving the inverse problem [19]. Modern devices allow obtaining a large amount of data. In order to refine the data statistics we formed from the experimental data several samples of transmittance spectra. With each sample of the transmittance spectrum, we solved the inverse problem taking into account the solutions obtained from other samples. In this way, we have achieved the convergence of the solutions for the most of the processed samples from the full set of transmittance spectra [20]. We have applied the previously published algorithms and program codes for solving the inverse problem [21] and used the data on the refractive index of metallic zinc given in [22]. The calculation of the kernel of the integral equation, while solving the inverse problem, was carried out with the program given in [23].

Figure 3b shows one of the graphs of the size distribution of dispersed Zn particles formed without a magnetic field. The horizontal segments correspond to the range of maxima of the size distributions, obtained from the various spectral dependences of the transmittance for given magnetic fields. The maxima of the size distribution functions of dispersed particles formed without a magnetic field in zinc vapor are in the range of 150-190 nm. The half-width of the distribution does not exceed 20 nm. The measured values of the maximum of this function in a magnetic field $B = 44$ mT are in the range of 160-170 nm, and in a field $B = 76$ mT in the range 180-190 nm. The distribution functions of dispersed particles in Fig. 3b and in Fig. 4 are displayed in relative units. Therefore, the amplitude of the maximum of all defined size distribution functions was taken as 100 units. In a magnetic field of 44 mT, the modal size does not exceed 160–170 nm, and in a field of 76 mT, 180–190 nm. Information on Zn particles with sizes less than 140 nm could not be obtained from data on the transmittance of optical radiation in the range 420-630 nm. This we attribute to the fact that the influence of the fine fraction of metallic Zn on the spectral course of transmittance is much less than that of the larger fraction due to both the factor of efficiency of interaction with optical radiation and the ratio of particle concentrations [24].
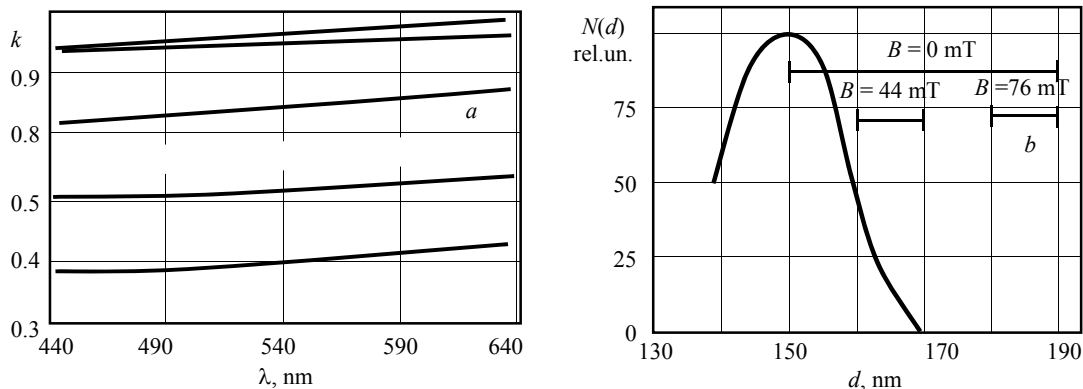
FIGURE 3. Results of optical diagnostics of a heterogeneous system: a) spectrum of transmittance of Zn particles in a magnetic field of 76 mT, b) dimensions of dispersed zinc particles formed in a magnetic field.

In the second facility, we deposited the dispersed particles of copper on glass substrates with aluminum coatings. On SEM images of dispersed particles with a magnification of 2,000 times we observed that the dispersed particles formed without a magnetic field had a wide range of sizes. Clusters of particles were visible on an area smaller than 3 microns. In some clusters, individual particles smaller than 250 nm were visible. Also visible were individual particles smaller than 300 nm. In a constant magnetic field of 30 mT, however, there was an insignificant number of clusters of particles in an area of less than 1 micron. We observed also a significant amount of individual particles smaller than 200 nm, see Fig. 4.

The SEM images of the deposited particles with magnification 5,000 with and without the magnetic field are shown in Fig. 4. In Fig. 4a we observe that the dispersed particles formed on the substrate without a magnetic field are grouped into conglomerates with smaller particles. In these conglomerates, individual particles of less than 250 nm are distinguished. In the clusters of particles obtained in a magnetic field of 30 mT, see Fig. 4b, there are individual particles with a size of less than 200 nm and multiple areas of the substrate with a size of less than 300 nm where the aluminum coating was removed. We expect that the metallic layer can be removed from the surface of the substrate in collisions with large hot particles characteristic for the arc discharge.
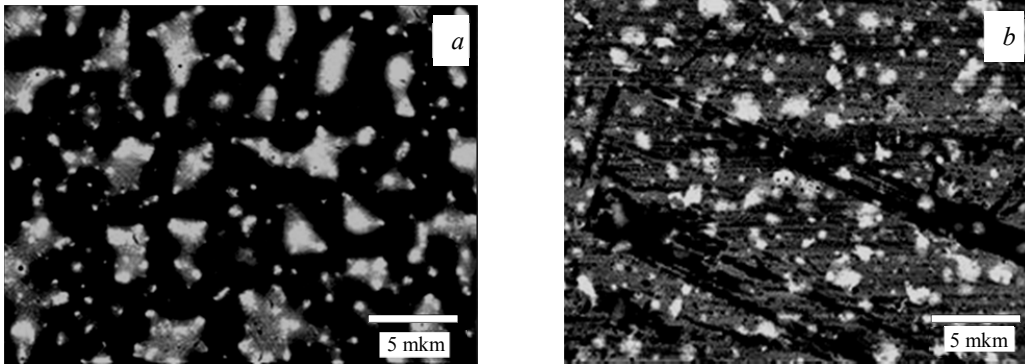
FIGURE 4. SEM images of copper particles (magnification 5,000 times) deposited from the arc plasma in a magnetic field: (a) $B = 0$ mT, (b) $B = 30$ mT.

With an increased magnification to 10,000 times a small number of damaged areas of the conducting layer of less than 80 nm are observed on the substrate also without a magnetic field. SEM images with a magnification of 60,000 times show individual particles about 10 nm in size, formed in the absence of magnetic field, and individual particles up to 40 nm in size, formed in a magnetic field. The particle size distribution, i.e. the granulometric composition, of dispersed Cu particles was determined by counting the number of particles of different sizes in SEM images. The data displays Fig. 5, lower curve. In a magnetic field of 30 mT the width of the size distribution function is significantly narrower.
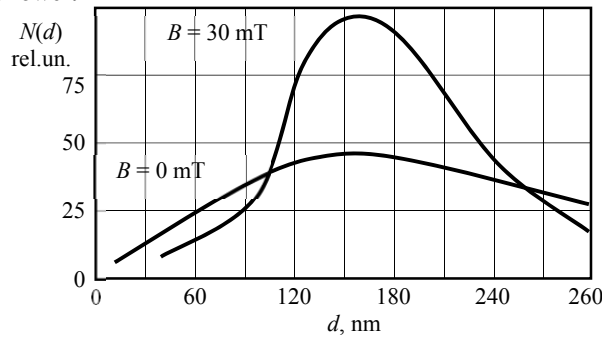
FIGURE 5. Dispersity of the Cu particles formed in the arc discharge facility without and with a magnetic field.

The dispersed particles of Cu are formed outside the arc discharge channel. Therefore, possible changes in plasma processes in a magnetic field do not affect the conditions of copper condensation.

A review of the experimental results shows the following. In a constant magnetic field of 44 or 76 mT, the granulometric composition of Zn nanoparticles formed from a high-temperature flow in the range of 100–200 nm is more uniform and stable over time than without a field. The range of change in the modal size distribution of

dispersed particles in size narrows to 160-170 nm in a magnetic field of 44 mT, and also shifts to 180-190 nm with an increase of the field to 76 mT.

SEM images show that without a magnetic field, much more conglomerates of Cu dispersed particles with a diameter of less than 300 nm are formed from high-temperature flux than in a field of 30 mT. In a magnetic field, we detect much more individual Cu particles with a diameter of less than 250 nm and less conglomerates than without a field.

The results observed experimentally can be explained as follows. The energy of magnetic interaction is much less than thermal energy. Therefore, in the above experiments, the magnetic field has practically no effect on the laws of the nucleation process determined by equations (1), (2). The increase in the size of dispersed particles can be represented as successive processes of sorption and formation of chemical bonds. The adsorption time of atoms on the surface of a solid (the molecules stay in the adsorbed state) depends on the adsorption heat of 1 mole of gas Q_a and is described by the Frenkel equation (3):

$$\tau_a \approx 10^{-13} e^{Q_a/RT}$$

(3)

Taking into account the maximum value of adsorption energy of 40 kJ/mol and the boiling point of Cu (2562°C) time of adsorption is measured as a 5.5×10^{-13} s; the similar assessment for Al (boiling point 2470°C) gives 5.7×10^{-13} s.

Cu, Zn are diamagnetics with magnetic susceptibility $\chi_{Cu} = -5.41 \times 10^{-6}$ and $\chi_{Zn} = -11.40 \times 10^{-6}$ respectively. As a rule, diamagnetics push out the external magnetic field. However, around a dispersed particle of diamagnetic material, the magnetic field will increase just slightly. For this reason, the influence of an external constant magnetic field on the process of nucleation is associated, in case of diamagnetic substances, with the influence on the spins of unpaired electrons of atomic particles from vapor and atoms residing on the free surface of dispersed particles. Both atoms from a gas and atoms on the surface of condensed particles have unpaired electrons. Without a magnetic field, the unpaired spins of the colliding particles in space haves a random orientation. The precession of the spins of valence electrons in a constant magnetic field reduces the number of possible spatial orientations of the two spins of colliding particles. From the formula for the Zeeman splitting of energy levels one can determine the time of the triplet-singlet conversion $\Delta t = h : (\mu_B g B)$ of the long-interacting spins. The estimates show that the time of triplet-singlet conversion allowing the transition of an atom from the sorbed state to the condensed state is 10^{-8}-10^{-6} s. By comparing this time with the adsorption time, we conclude that the dynamics of spin pairs on the surface of dispersed particles or condensation nuclei cannot have a significant effect on the nucleation process.

The uncertainty relation for the spin projections on the coordinate axes reads: $\Delta S_x \Delta S_y \geq h/2|\langle S_z \rangle|$ [25]. By using this relation it can be shown, that the first collision of radicals in a magnetic field due to the thermal motion in the conditions of thermodynamic equilibrium of the spin system, only the $1/(3n)$ part (singlet state) [10] ends with the formation of molecules. Here n represents the number of non-overlapping phase uncertainty ranges of spin precession. This relationship will also be satisfied when an atom collides with a cluster or a dispersed particle. At high temperatures, an atom may diffuse for some time along the surface of the condensed phase. In this case, an atom colliding with the surface may return to the vapor phase or become part of the condensed phase.

Without an external magnetic field, assuming that each of the two radicals under consideration is in the magnetic field of the other radical, the probability of the formation of a singlet state at the first collision is $(3n)^{-3}$. Therefore, it should be expected that in an external constant magnetic field the probability of the formation of a singlet pair at the first collision will increase by $(3n)^2$ times, compared to the value without a field. In [10] it was shown that $(3n)^2 > 36$. At the same time, the frequency of nuclei formation of a new phase and the coefficient of desublimation increase. The desublimation coefficient takes into account both the influence of the dynamics of spin pairs of atoms from the gas phase and on the surface of a dispersed particle, as well as the relaxation rate of the released energy of the chemical bond.

During nucleation of supersaturated vapors of Zn and Cu in the magnetic field the rate of formation of condensation nuclei as well as the probability of reaching a critical size increases. In the magnetic field, the dispersed particles Zn or Cu also grow faster than without the field. As a result, the degree of vapor supersaturation decreases faster to the level at which the formation of new condensation nuclei ceases. Therefore, the concentration of dispersed particles, in the region of size distribution function that describes small-sized particles, is significantly reduced.

The formation of condensation centers and cluster growth at the initial stage of nucleation in a magnetic field is largely determined by spin interactions. For a fine fraction of dispersed particles, due to the slight slip relative to the gas flow, a region of desiccation of supersaturated steam forms around the particles, separating the two growing

particles. Under these conditions, the growth rate of particles is determined not by magnetic phenomena, but by the diffusion of atoms from the vapor phase to the surface. As the diameter of the dispersed particles increases, they begin to lag behind the gas flow. The vapor-depleted diffusion shell disappears. As a result, the growth of a larger fraction begins to be influenced by a constant magnetic field again.

CONCLUSION

We studied experimentally the condensation of Zn and Cu vapors from a high-temperature gas in an external weak constant magnetic field. The sizes of Zn particles were estimated from laser probing data, and those of the Cu particles from SEM images of a deposited layer on a substrate. We observed at all applied conditions, a chaotic time shift of the maximum of the size distribution function of dispersed particles. For example, without a magnetic field, the maximum of the particle size distribution function Zn varied in the range 150-190 nm, in the field 44 mT in the range 160-170 nm, and in the field 76 mT in the range 180-190 nm. Simultaneously, we noted a decrease in the width of the size distribution function of dispersed particles of Zn from 40 nm (0 mT) to 10 nm (44 mT or 76 mT) in an applied magnetic field and the displacement of the maximum of the size distribution function towards larger sizes with increasing magnetic field. The sizes of the dispersed Cu particles, determined as a value averaged over the deposition time, were found in the range of 10-400 nm without a magnetic field, and in the range of 30-320 nm in the magnetic field of 30 mT. We relate the observed results to the arrangement of the dynamics of spin pairs of unpaired electrons of the atom from the gas phase and the atom located on the surface of condensed particles that occurs in an applied magnetic field. On that account, in a magnetic field increases the probability of forming a singlet spin pair that in turn facilitates joining to the dispersed phase when an atom from the gas phase first collides with the dispersed particle or condensation nucleus.

ACKNOWLEDGMENT

REFERENCES

1. A.L. Daltin and M. Benaissa, J.P. IOP Conf. Ser.: Mater. Scie. Eng. **424**, 012022 (2018).
2. C. Liu, A. Tian, H. Yang, Q. Xu and X. Xue Appl. Surf. Sci. **287,** 218–222 (2013).
3. L. Gang, Surf. Rev. Lett. **25**, 4 1850037 (2018).
4. A. Bund and A. Ispas ECS Transact. **13** (16), 1–7 (2008).
5. C.J. Li, H. Yang, Z.M. Ren, W.L. Ren and Y. Q. Wu, Progress In Electromagnetics Research Letters **15**, 45–52 (2010).
6. A.A. Serkov, Appl. Phys. Lett. **109**, 053107 (2016).
7. Y. Arita, M. Ploschner, M. Antkowiak, F. Gunn-Moore and K. Dholakia, Opt. Lett., **38**(17), 3402–3405 (2013).
8. K.K. Kim, M. Roy, H. Kwon, J.K. Song and S.M. Park, J. Appl. Phys. **117**(7), 074302 (2015).
9. T.E. Itina, J. Phys. Chem. C **115**(12), 5044–5048 (2010).
10. V.F. Myshkin, E.V. Bespala, V.A. Khan and S.V. Makarevich IOP Conf.Ser. Mater. Sci. Eng. **135**, 012029 (2016).
11. V.I. Vishnyakov, S.A. Kiro, M.V. Oprya and A.A. Ennan, Physics of Aerodispersed Systems, (**51**) 87–98 (2014).
12. V.A. Pavlov and V. P. Skripov, High Temperature, **8**(3) 540–545 (1970) (in Russian).
13. A.G. Amelin, *Theoretical Basis of the Formation of Fog During Vapor Condensation* (Chemistry, Moscow, 1972) p.304 (in Russian).
14. A.G. Gorelik and A.V. Amitin, *Desublimation in the Chemical Industry* (Chemistry, Moscow, 1986) p.272.
15. Yu.Yu. Lutsenko, J. Technical Physics **75** (11) 124-126 (2005) (in Russia)
16. O.G. Volokitin, G.G. Volokitin, N.K. Skripnikova and V. Shekhovtsov, AIP Conf. Proc. **1698**, 070022 (2016).
17. A.G. Karengin, A.A. Karengin, O.D. Podgornaya and E. E. Shlotgauer IOP Conf. Ser.: Mater. Sci. Eng. **66,** 12034 (2014).
18. L.I. Dorofeeva and D. Orekhov, AIP Conf. Proc. **1938**, 020011 (2018).
19. V.E. Zuev and I.E. Naats *Inverse Problems of Lidar Sensing of the Atmosphere* (Springer-Verlag, Berlin, 1983) p. 262.
20. X. Lai, Y. Zheng, H. Ipsen, S. Jacobsen, J.N. Larsen, H. Lowenstein and I. Sondergaard, Appl. Spectrosc. **61**(11), 1184–1190 (2007).
21. V.I. Gelfgat, E.L. Kosarev, E.R. Podolyak, Comput. Phys. Commun. **74**(3) 349–357 (1993).
22. W.S.M. Werner, K. Glantschning and C. Ambrosch-Draxl, J. Phys. Chem. Ref. Data **38** 1013–1096 (2009).
23. van de Hulst H.C. *Light Scattering by Small Particles* (Dover, New York, 1981).
24. V.F. Myshkin, D.A. Izhoykin, A.S. Grigoriev, D.L. Gamov and D.A. Leonteva, AIP Conf. Proc. **1938**, 020012 (2018).
25. D. H. McIntyre, *Quantum Mechanics: a Paradigms Approach* (Pearson Addison-Wesley, San Francisco, 2012) p.598.